TERAHERTZ SPECTROSCOPY AND MOLECULAR MODELING OF BARBITURIC ACID

Zh. Zheng*, Ch. Li, J. Dong, Sh. Zhou

School of Electronic Engineering at Xi'an University of Posts&Telecommunication, Xi'an 710121, China; e-mail: zhengzhuanp@xupt.edu.cn

The well-resolved terahertz (THz) absorption spectrum of barbituric acid has been investigated using terahertz time-domain spectroscopy. Four distinct THz spectral features and two shoulder peaks were observed in the range of 10–124 cm^{-1}. A complete analysis was performed with density functional theory, which provided an excellent agreement between solid-state simulation and experiment. The solid-state analysis indicates that the six experimental spectral features observed at low temperature consist of nine infrared-active vibrational modes. Further simulations based on hydrogen-bond isotopologues were performed to study the involvement of hydrogen bonds in the collective modes. A feature at 118.0 cm^{-1} mainly stems from the collective vibration of dimer hydrogen bonds (m) while features at 102.0 and 109.6 cm^{-1} primarily come from the collective vibrations of linear hydrogen bonds (n). The results may be useful for monitoring molecular reaction in industrial production according to the state of hydrogen bonds.

Keywords: *terahertz time-domain spectroscopy, simulation, barbituric acid, density functional theory, hydrogen bond.*

ИССЛЕДОВАНИЕ БАРБИТУРОВОЙ КИСЛОТЫ С ИСПОЛЬЗОВАНИЕМ ТЕРАГЕРЦОВОЙ СПЕКТРОСКОПИИ И МОЛЕКУЛЯРНОГО МОДЕЛИРОВАНИЯ

Zh. Zheng*, Ch. Li, J. Dong, Sh. Zhou

УДК 535.34:547.854.5

Школа электронной инженерии Сианьского университета почты и телекоммуникаций, Сиань 710121, Китай; e-mail: zhengzhuanp@xupt.edu.cn

(Поступила 2 декабря 2019)

С помощью терагерцовой спектроскопии во временной области исследован спектр ТГц-поглощения барбитуровой кислоты. В диапазоне 10–124 $см^{-1}$ наблюдались четыре отчетливые спектральные терагерцовые особенности и два плечевых пика. Полный анализ выполнен с помощью теории функционала плотности, которая обеспечила согласие между твердотельным моделированием и экспериментом. Показано, что шесть экспериментальных спектральных особенностей, наблюдаемых при низкой температуре, состоят из девяти ИК активных колебательных мод. Дальнейшее моделирование на основе изотопов водородных связей выполнено для изучения участия водородных связей в коллективных модах. Особенность при 118.0 $см^{-1}$ в основном связана с коллективным колебанием водородных связей димера (m), в то время как при 102.0 и 109.6 $см^{-1}$ — с коллективными колебаниями линейных водородных связей (n). Результаты могут быть полезны для мониторинга молекулярной реакции в промышленном производстве по состоянию водородных связей.

Ключевые слова: *терагерцовая спектроскопия во временной области, моделирование, барбитуровая кислота, теория функционала плотности, водородная связь.*

Introduction. With the advent of ultra-fast pulse lasers and the development of semi-insulating semiconductors, there has been significant progress in terahertz (THz) technologies [1]. The rapid development has allowed researchers to shift their focus to THz applications [2–4]. Because the frequency window is 0.1–10 THz, THz waves have bridged the gap between electronics and photonics. Thus, THz spectroscopy has been used to probe lattice optical phonon modes and provide spectral information specific to the crystal-

line lattice [5]. It has recently become widely used in other applications [6–8], such as the identification of polymorphs in pharmaceuticals [7] and the detection of explosives [8].

However, the observed THz spectral features are only useful if there is a high level of confidence in the interpretation. The understanding of the features is a crucial point for extracting information on spectral origins. To date, research has shown that experimental band assignments can be accomplished via density functional theory (DFT) [9–11]. For example, Takahashi et al. used DFT to successfully acquire low-frequency vibrational information on nicotinamide [10]. By using DFT, observed THz absorption features could provide precise information of molecular interactions.

Barbituric acid (pyrimidine-2,4,6-trione), an organic compound based on a pyrimidine heterocyclic skeleton, with the appearance of white crystals, can form a large variety of barbiturate drugs that behave as central nervous system depressants. It is also one of four ingredients used to make vitamin B_2. Vibrational information on materials may possibly shed light on their biological implications [12, 13]. The infrared (IR) spectrum of barbituric acid only have been reported [14, 15], but very little is known about its lowest-frequency vibrational motions, especially molecular interactions in THz region. This is particularly important for molecular reactions and environmental protection [10].

Here, THz time-domain spectroscopy (THz-TDS) was used to measure the room temperature (RT) spectrum of barbituric acid over the range of 10–124 cm^{-1}. DFT, a useful method of quantum mechanics for vibrational analysis, was employed to predict the origins of the experimental features. Based on the good agreement between the experimental and calculated spectra, a complete vibrational assignment is discussed. DFT simulations based on hydrogen-bond (N-H···O) isotopologues were also performed to exploit its precise intermolecular motions.

Experimental and theoretical methods. THz spectrum (10–124 cm^{-1}) was acquired using a CIP-TDS THz-TDS system (Daheng Optics, China) with resolution of 2.0 cm^{-1}. The instrument used a photoconductive antenna system to generate and detect THz radiation, which was excited by femtosecond pulses at 800 nm, 100 fs from a mode-locked titanium sapphire laser at a repetition rate of 80 MHz. Figure 1 shows the THz-TDS spectral system.

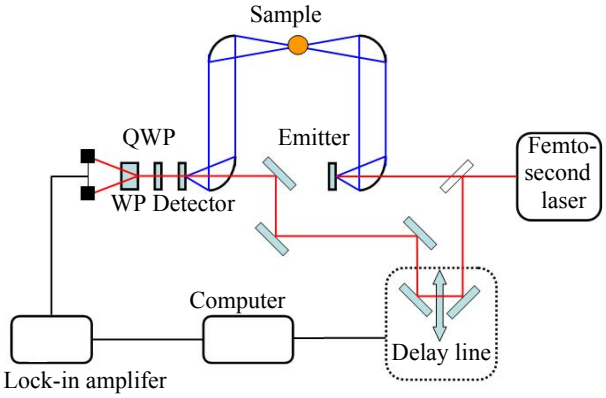

Fig. 1. The Terahertz time-domain spectral system.

Barbituric acid (CAS-number: 67-52-7) was acquired from Chengdu Chemical Reagent Co. Ltd. It was analytical grade (>99%) and used without further purification. The sample was first crushed into a fine powder with a mortar and pestle to minimize particle scattering. Then, it was mixed with polytetrafluoroethene (PTFE) powder in mass ratios of 1:3 and compressed into 1.3-mm-thick pellets at a pressure of 800 kg/cm^2.

Theoretical, calculations for periodic systems were based on plane-wave DFT methods within the generalized gradient approximation (GGA) [16]. Norm conserving pseudopotentials in the Kleinman-Bylander form [17] were used, and all calculations employed the Perdew-Burke-Ernzerhof functional [18]. The total energy converged to 10^{-8} eV/atom and the maximum forces between atoms were less than 10^{-5} eV/Å. A plane wave cutoff energy of 1200 eV was used. The THz vibrational frequencies were acquired from the normal mode eigenvalues of the mass-weighted Hessian. The atomic coordinates were optimized with the fixed unit cell. Specifically, the crystal cell parameters were used for RT $P2_1/c$ (Z = 4) [19], a = 6.817 Å, b = 14.310 Å, c = 6.248 Å, α, γ = 90.0°, β = 118.57°, V = 535.284 $Å^3$. Figure 2 shows the molecular structure and the crystalline arrangement of barbituric acid.

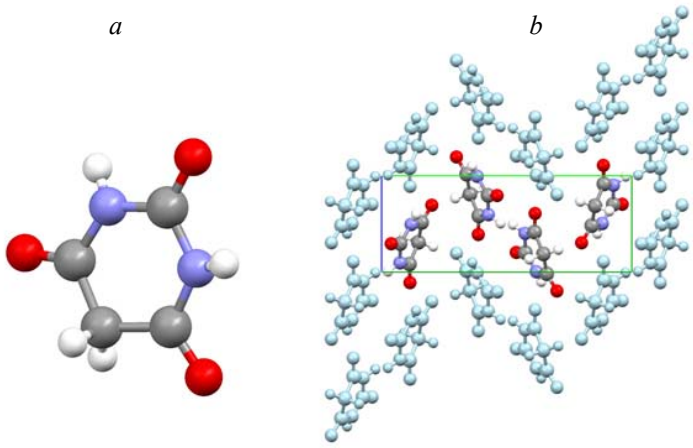

Fig. 2. The molecular structure (a) and crystal molecular arrangement (b) of barbituric acid.

Results and discussion. RT (295 K) THz spectral features of barbituric acid are shown in Fig. 3. Four sharp absorption features and two shoulder peaks were observed over the range of 10–124 cm^{-1}. Specifically, the spectrum has four distinct features at 60.0, 82.6, 102.0, and 118.0 cm^{-1}. The highest-intensity feature occurred at 102.0 cm^{-1} with two shoulder peaks located at 91.9 and 109.6 cm^{-1}. The second most intense feature was at 82.6 cm^{-1}, and the two medium-intensity features were located at 60.0 and 118.0 cm^{-1}.

According to its molecular structure, barbituric acid has thirteen atoms with no symmetry. Thus 33 intramolecular vibrational modes of the molecule are expected to be IR active. Because each unit cell contains four molecules ($Z = 4$), barbituric acid therefore has a total of 153 optical modes, 132 are intra-molecular vibrations and 21 ($4B_u+5A_u+6A_g+6B_g$) can be attributed to intermolecular phonons. The point group of the unit cell has C_{2h} symmetry, thus optical modes with Au and Bu symmetries are only infrared active.

Isolated-molecule DFT was initially performed to analyze the experimental features. Only one mode located at 11.2 cm^{-1} was obtained over the range of 10–124 cm^{-1}, in contrast to the observed peaks in the experimental spectrum. This result indicates that intramolecular motion has no contribution in the experimental spectrum. It also implies that isolated-molecule theory failed to interpret the molecular system, as also reported elsewhere [6, 11].

Because of the failure of the isolated-molecule simulation, solid-state theory with the unit cell as the starting point was performed. Figure 4 shows the solid-state simulation result along with the experimental features. In this case, the calculations exhibited a high degree of fitting. Because three modes were of very low intensity, six calculated modes were mainly used to analyze the experimental features. Specifically, the calculated mode at 55.4 cm^{-1} was used to understand the feature at 60.0 cm^{-1}, the mode at 77.7 cm^{-1} corresponded to the observed feature at 82.6 cm^{-1}, the experimental absorption at 91.9 cm^{-1} was assigned to the calculated mode at 94.3 cm^{-1}, and the two calculated modes at 102.0 and 118.0 cm^{-1} were likely responsible for the two experimental features at 102.6 and 118.1 cm^{-1}, respectively. The last remaining calculated mode at 104.9 cm^{-1} can be used to interpret the shoulder peak at 109.6 cm^{-1}. Table 1 lists the experimental and calculated THz spectral data. Based on the assignments, the THz experimental spectral features could be perfectly modeled by the solid-state theory.

Discrepancies remain between the experimental peaks and calculated results. The mode at 65.5 cm^{-1} was calculated in a region in which no absorption was observed in the experimental spectrum. It may coincide with the modes contributing to the experimental feature at 60.0 cm^{-1}, or it is possible that the calculated intensity was overestimated. Furthermore, there are discrepancies between the calculated and experimental absorption intensities. Calculated spectral intensities may sometimes be improved by a using larger cutoff energy and an appropriate correlation functional. Table 1 provides the detailed assignments based on the comparison of the experimental and simulation results. Descriptions of each mode were made by vision inspection of the atomic displacements and are based on the most significant contributions to the vibrational mode character.

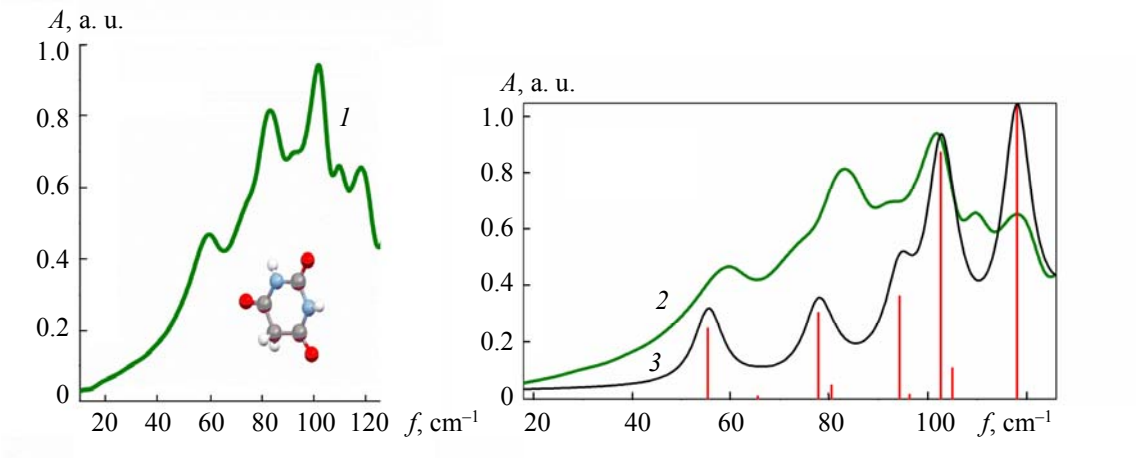

Fig. 3. The measured (1) and experimental (2) THz spectral features and solid-state calculated result (3) for barbituric acid.

TABLE 1. Experimental Features (cm^{-1}) and Calculated Modes for Barbituric Acid

Experimental	Calculation	
RT	PBE	Description
60.0	55.4(0.88)	Lattice mode (translation)
	65.5(0.01)	Lattice mode (rotation)
82.6	77.7(0.30)	Lattice mode (rotation)
	80.4(0.05)	Lattice mode (rotation)
91.9	94.3(0.36)	Lattice mode (rotation)
	96.3(0.02)	Interdimer rotation
102.0	102.6(0.88)	Interdimer translation
109.6	104.9(0.11)	Interdimer translation
118.0	118.1(1.04)	Butterfly

N o t e. Infrared intensities (km/mol) are shown in parentheses.

According to the molecular arrangement, one barbituric acid molecule can form four hydrogen bonds with others [19]. However, two of them are in the same value and purpose. One hydrogen bond (*m*) with a length of 2.903 Å (N-H···O) is used to link the dimer form, while another (*n*) with a length of 2.795 Å (N-H···O) is used to link neighboring molecules in line. Figure 4 shows the hydrogen bond network of barbituric acid. To study the involvement of two kinds of hydrogen bonds in the collective modes, we used solid-state calculations to simulate hydrogen-bond isotopologues. Specifically, the dimer hydrogen bond (*m*) and two types of hydrogen bonds (*m*, *n*) were separately simulated, with the isotopic substitution of the bond from N^{14}-H^{1}···O^{16} to N^{15}-D^{2}···O^{18}. The calculated results are provided in Figs. 5b,c along with the unchanged simulation result in Fig. 5a. The overall isotopic change of N-H···O was made to obtain a clear spectral shift and to make the contributions of van der Waals forces and hydrogen bonds clear.

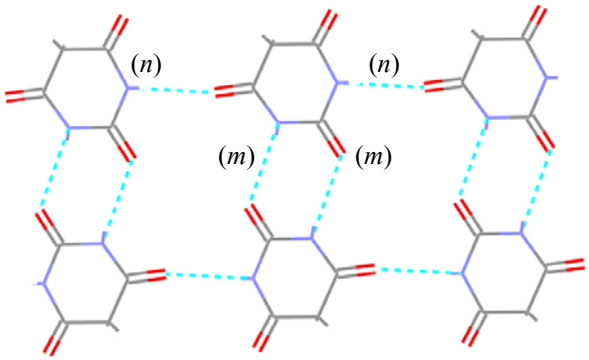

Fig. 4. The image of hydrogen bonds among barbituric acid molecules.

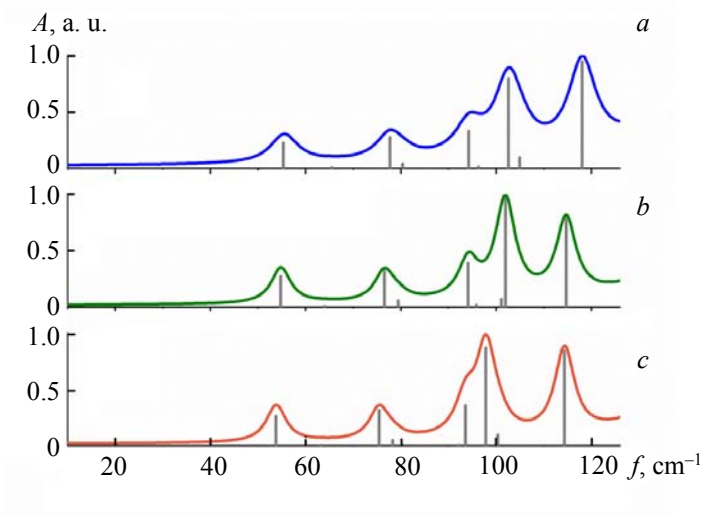

Fig. 5. The calculated absorption spectra for barbituric acid (a), the dimer hydrogen bond isotopologues (b), and all hydrogen bonds isotopologues (c).

As shown in Fig. 5, the absorption peaks shift to low frequency as the molecular mass increased [15]. Compared with that shown in Figs. 5a,b, there is a large shift in the last mode, from 118.1 to 114.7 cm^{-1}. However, this peak has only a 0.4 cm^{-1} difference in Fig. 5c. A possible reason is that this mode mainly originates from the collective vibration of dimer hydrogen bonds (m), compared to that of the small contribution of the linear hydrogen bond (*n*). Comparison of Figs. 5a,c shows three modes showing big shift, 96.3 cm^{-1} changes to 93.6, 102.6 cm^{-1} changes to 97.8 and 104.9 cm^{-1} changes to 100.3 cm^{-1}. The possible explanation is that these three modes primarily come from collective vibrations of linear hydrogen bond (*n*). Because the remaining modes shown in Figs. 5b,c change at the same level, they most likely derive from lattice rotation and translation. Table 2 gives the calculated data that provide more information for barbituric acid intermolecular interactions and clarify the assignments. Thus, it can be estimated that the feature at 118.0 cm^{-1} mainly stems from the collective vibrations of dimer hydrogen bonds (*m*), while the features at 102.0 and 109.6 cm^{-1} mainly come from collective vibrations of linear hydrogen bonds (*n*). Further, the peak at 91.9 cm^{-1} primarily results from the combination of van der Waals forces and hydrogen bond (*n*). The remaining features mainly originate from van der Waals forces.

TABLE 2. The Calculated Modes (cm^{-1}) for Barbituric Acid and its Isotopologues

Barbituric acid	Isotopologues	
55.4(2.97)	54.8(2.93)	53.8(2.89)
65.5(0.11)	64.0(0.08)	63.1(0.04)
77.7(3.65)	76.6(3.48)	75.4(3.47)
80.4(0.55)	79.5(0.61)	78.3(0.54)
94.3(4.36)	94.1(4.22)	92.2(0.04)
96.3(0.19)	95.9(0.19)	93.6(3.91)
102.6(10.51)	101.1(0.76)	97.8(9.56)
104.9(0.29)	102.0(10.52)	100.3(1.07)
118.1(12.63)	114.7(8.79)	114.3(9.28)

N o t e. Infrared intensities (km/mol) are shown in parentheses.

Conclusions. We have investigated the THz absorption spectrum of barbituric acid using THz-TDS. Four distinct spectral features located at 60.0, 82.6, 102.0, 118.0 cm^{-1}, and two shoulder peaks lying at 91.9 and 109.6 cm^{-1} have been acquired in the range of 10–124 cm^{-1}. DFT was used to interpret the experimental features and a nearly realistic description of the experimental THz spectrum was obtained. Peak assignments implied that all observed features derived from intermolecular forces. Moreover, the involvement of hydrogen bonds in collective modes was also investigated using hydrogen-bond isotopologues simulations. The

solid-state analysis indicated that the feature at 118.0 cm^{-1} mainly stems from the collective vibrations of dimer hydrogen bonds (*m*), the features at 102.0 and 109.6 cm^{-1} mainly result from collective vibrations of hydrogen bonds (*n*), and the peak at 91.9 cm^{-1} primarily results from the combination of van der Waals forces and the hydrogen bond (*n*). Overall, these results may be useful for monitoring molecular reactions in industrial production.

Acknowledgements. This work was supported by the National Science Foundation for Young Scientists of China (Grant No. 11604263) and the education department of Shaanxi Province (Grant No. 16JK1698).

REFERENCES

1. D. Dragoman, M. Dragoman, *Prog. Quantum Electron*., **28**, 1–66 (2004).
2. M. Mizuno, A. Y. Kaori, *J. Biol. Phys*., **41**, 293–301 (2015).
3. Z. X. Li, J. Zhou, X. S. Guo, B. B. Ji, W. Zhou, D. H. Li, *J. Appl. Spectrosc.*, **85**, No. 5, 840–844 (2018)
4. X. Wu, Y. X. Xu, L. Wang, *Appl. Phys. Lett.*, **101**, 033704 (2012).
5. M. D. King, W. Ouellette, T. M. Korter, *J. Phys. Chem*., **115**, 9467–9478 (2011).
6. L. Liu, L. Shen, F. Yang, F. Han, P. Hu, M. Song, *J. Appl. Spectrosc.*, **83**, 603–609 (2016).
7. M. D. King, W. D. Buchanan, *J. Pharm. Sci*., **83**, 3786–3792 (2011).
8. C. T. Konek, B. P. Mason, J. P. Hooper, C. A. Stoltz, J. Wilkinson, *Chem. Phys. Lett*., **489**, 48–53 (2010).
9. P. M. Hakey, D. G. Allis, M. R. Hudson, W. Ouellette, T. M. Korter, *Chem. Phys. Chem*., **10**, 2434–2444 (2009).
10. M. Takahashi, N. Okamura, X. Fan, H. Shirakawa, H. Minamide, *J. Phys. Chem. A*, **121**, 2558–2564 (2017).
11. C. Oppenheim, T. M. Korter, J. S. Melinger, D. R. Grischkowsky, *J. Phys. Chem. A*, **114**, 12513–12521 (2010).
12. J. Dong, Z. Zhang, H. Zheng, M. Sun, *Nanophotonics*, **4**, 472–490 (2015).
13. B. Lei, J. Wang, J. Li, J. Tang, Y. Wang, W. Zhao, Y. Duan, *Opt. Express*, **27**, 20541–20557 (2019).
14. A. J. Barnes, L. L. Gall, J. Lauransan, *J. Mol. Struct.*, **56**, 29–39 (1979).
15. S. Sebastian, H. T. Varghese, Y. S. Mary, C. Y. Panicker, *Orient. J. Chem*., **26**, 1139–1142 (2010).
16. S. J. Clark, M. D. Segall, C. J. Pickard, P. J. Hasnip, M. J. Probert, K. Refson, M. C. Payne, *Z. Kristallogr*., **220**, 567–570 (2005).
17. L. Kleinman, D. M. Bylander, *Phys. Rev. Lett.*, **48**, 1425 (1982).
18. J. P. Perdew, J. A. Chevary, S. H. Vosko, K. A. Jackson, M. R. Pederson, D. J. Singh, C. Fionlhais, *Phys. Rev. B*, **46**, 6671–6687 (1992).
19. T. C. Lewis, D. A. Tocher, S. L. Price, *Cryst. Growth Des.*, **4**, 979–987 (2004).